University of
Technology
Sarawak

**ORIGINAL ARTICLE**

# Compressive Behaviour of Concrete-Filled Plastic Tubes with Hybrid Steel and E-glass Fibre Reinforcement

*Jen Hua Ling and Richard Jia Li Ling

¹Centre for Research of Innovation & Sustainable Development, School of Engineering and Technology, University of Technology Sarawak, 96000 Sibu, Sarawak, Malaysia

**ABSTRACT** - This study examined the compressive behaviour of concrete-filled plastic tubes (CFPT) made with PVC tubes and fibre-reinforced concrete (FRC). Steel and E-glass fibres were added at 0%, 0.75%, and 1.5% by cement weight, both individually and in combination, to assess their effect on structural performance. A total of 54 cylindrical specimens were tested in four groups: plain concrete (C), fibre-reinforced concrete (FC), concrete-filled PVC tubes (TC), and fibre-reinforced concrete-filled PVC tubes (FTC). All specimens were cast in PVC tubes (150 mm diameter × 305 mm height), cured for 28 days, and tested under axial compression using a Universal Testing Machine. The results showed that fibre addition generally reduced compressive strength, especially in unconfined specimens. E-glass fibres had a stronger negative impact than steel fibres, with up to 49.6% strength loss at 1.5% E-glass content. Only one specimen (FTC-2 with 1.5% steel fibres) showed a slight strength increase of 2.7%. Hybrid fibre reinforcement showed limited effectiveness under the present mix conditions, likely due to poor fibre dispersion and low workability. PVC tube confinement exhibited mixed results, possibly due to the tubes' low tensile strength and thin walls. Overall, the findings suggest that under low-workability conditions, hybrid fibres may not fully enhance compressive strength. Further research is needed to improve workability, fibre dispersion, and bonding, and to optimise fibre dosage.

## INTRODUCTION

Concrete-filled tubes (CFTs) are composite structural elements consisting of hollow tubes filled with concrete [1]. They are commonly used in high-rise buildings, bridges, tunnels, subways, towers, and offshore structures [2-3].

CFTs perform well under compression. The concrete carries the compressive load, while the tube provides external confinement and reinforcement, eliminating the need for internal reinforcement. The tube limits lateral expansion of the concrete, and the concrete supports the tube against buckling [4]. This interaction results in a combined strength greater than the sum of each material alone [5]. CFTs are also easy to construct. The tube acts as stay-in-place formwork, supporting fresh concrete during casting and removing the need for formwork removal, which speeds up construction [2; 6-7].

Concrete-filled steel tubes (CFST) are the most common form of CFT. They offer high compressive strength, seismic resistance, ductility, and energy absorption [2; 8]. However, steel tubes are prone to corrosion, especially in marine, limiting their long-term durability [9-10]. Protective coatings can help but are often unreliable over time or with poor maintenance [11].

To overcome corrosion issues, fibre-reinforced polymer (FRP) tubes are used in Concrete-Filled FRP Tubes (CFFT) as corrosion-resistant alternatives [12-15]. FRPs offer high strength-to-weight ratios [16-17] and resist chloride-induced corrosion [18]. However, their high material and labour costs [19] and brittle failure [6] have limited their widespread use. FRPs are good in tensile strength but inferior in compression

[20]. While they confine concrete effectively, they carry limited axial load [21]. In comparison, CFSTs use steel tubes that provide both strong confinement and axial strength.

Concrete-Filled Plastic Tubes (CFPT) have emerged as cost-effective, corrosion-resistant alternatives. Commonly used plastics include polyvinyl chloride (PVC), unplasticized PVC (uPVC), and high-density polyethylene (HDPE). These materials are lightweight, inexpensive, easy to install, widely available, durable, and resistant to corrosion [1]. However, these materials have low stiffness and strength. For example, PVC's modulus of elasticity is about 1/50th that of steel [22], resulting in limited confinement and lower axial load resistance.

To address this limitation, this study explores the use of fibre-reinforced concrete (FRC) inside PVC tubes. Fibres can enhance concrete's tensile strength, ductility, toughness, and durability [23]. Steel fibres, in particular, provide an effective and economical way to enhance ductility in CFST columns compared with thicker steel tube [24].

Fibres vary in strength and stiffness. High-modulus, high-strength fibres like carbon, polyvinyl alcohol, steel, asbestos, and glass enhance concrete strength, while lower-strength fibres such as nylon, acrylic, and polypropylene help control cracking and improve ductility [23]. This study used steel and E-glass fibres for their high strength and stiffness. Although PVC tubes offer some protection, steel fibres still face long-term corrosion risks. To reduce this concern while maintaining performance, E-glass fibres were used to partially replace steel fibres.

While most FRC uses a single fibre type [23], combining fibres with different properties can offer complementary benefits. Each type may enhance specific concrete properties [25], and no single fibre provides all the desired mechanical characteristics [26]. Previous studies on hybrid FRC have mainly focused on combinations of steel and polypropylene fibres [25-26], with limited application CFPT.

This study contributes experimental data on the compressive behaviour of concrete-filled PVC tubes incorporating steel, E-glass, and hybrid fibres. The work examines how fibre addition interacts with the limited confinement provided by plastic tubes, clarifying the challenges of combining fibre reinforcement with low-stiffness confinement. The findings provide practical insight into the performance limits and design considerations for cost-effective, corrosion-resistant CFPT systems.

## MATERIALS AND METHODOLOGY

### Specimen Details

A total of 54 specimens, each 305 ± 5 mm in height, were prepared and divided into two groups: with PVC tubes (CFPTs) and without PVC tubes (concrete cylinders), as shown in Figure 1. The PVC tubes had an internal diameter of 155 mm and a wall thickness of 2 mm. Each group used two types of concrete: plain and fibre-reinforced, resulting in four specimen types:
- C: Plain concrete
- FC: Fibre-reinforced concrete (FRC)
- TC: Concrete-filled PVC tubes
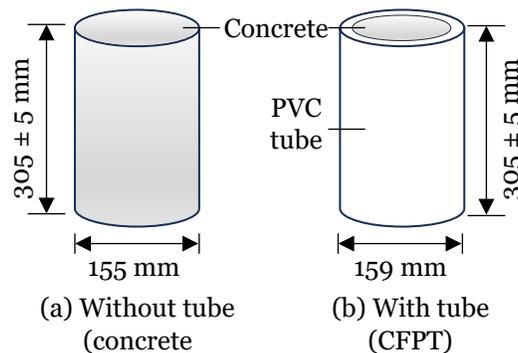- FTC: Fibre-reinforced concrete-filled PVC tubes



**Figure 1.** Geometrical dimensions of the test specimens.

The comparison strategy was as follows:
- C vs FC: To evaluate the effect of steel and/or E-glass fibres without PVC tube confinement
- TC vs FTC: To evaluate the effect of steel and/or E-glass fibres with PVC tube confinement
- C vs TC: To determine the effect of PVC tube confinement on plain concrete
- FC vs FTC: To determine the effect of PVC tube confinement on fibre-reinforced concrete

Two variables were studied: steel fibre content (0%, 0.75%, and 1.5%) and E-glass fibre content (0%, 0.75%, and 1.5%). Specimen configurations are listed in Table 1.

**Table 1.** Details of specimen

| E-glass fibre content | Without PVC tube | | | With PVC tube | | |
|---|---|---|---|---|---|---|
| | Steel fibre content | | | Steel fibre content | | |
| | 0% | 0.75% | 1.5% | 0% | 0.75% | 1.5% |
| 0% | C-1 | FC-1 | FC-2 | TC-1 | FTC-1 | FTC-2 |
| 0.75% | FC-3 | FC-5 | FC-7 | FTC-3 | FTC-5 | FTC-7 |
| 1.5% | FC-4 | FC-6 | FC-8 | FTC-4 | FTC-6 | FTC-8 |

Notes: Each configuration includes 3 identical specimens, totalling 27 specimens with PVC tubes and 27 without.

## Specimen Fabrication

Grade 25 concrete with a water-to-cement (w/c) ratio of 0.58 was used. The mix proportion is presented in Table 2. Ordinary Portland Cement (OPC) grade 42.5 served as the binder. Coarse aggregate was granite sized between 6.3 mm and 20 mm, while river sand passing a 600 μm sieve was used as fine aggregate. Both aggregates were oven-dried at 105°C for 24 hours before mixing to maintain a consistent w/c ratio. The mixing process is illustrated in Figure 2.



(a) Oven-drying aggregates  (b) Sieving aggregates  (c) Weighting materials  (d) Mixing materials using a mixer  (e) Adding water and superplasticizer  (f) Compacting cube sample

**Figure 2.** Concrete mixing and specimen preparation process.

**Table 2.** Concrete mix proportions used

| Material | Weight per meter cube of concrete |
|---|---|
| Cement | 328 kg/m$^3$ |
| Water | 196 kg/m$^3$ |
| Fine aggregate | 688 kg/m$^3$ |
| Coarse aggregate | 1224 kg/m$^3$ |

**Table 3.** Physical and mechanical properties of reinforcing fibres.

| Property | Steel Fibre | E-glass Fibre |
|---|---|---|
| Type | Hooked-end | Chopped strands |
| Length | 35 mm (±1.75 mm) | 6 mm |
| Diameter | 0.55 mm (±0.03 mm) | - |
| Minimum Tensile Strength | ≥ 1200 N/mm² | - |

A superplasticizer (Real Power Flow RPF 630) was added at 0.5% of the cement weight to improve workability. Steel and E-glass fibres were added at 0%, 0.75%, and 1.5% by weight of cement. Fibre specifications are shown in Table 3.

Concrete was cast in batches based on the fibre combinations. Cement, sand, coarse aggregate, and fibres (if included) were dry mixed first, followed by the addition of water and superplasticizer.

PVC tubes served as casting moulds for all specimens. Concrete was poured in three equal layers, with each layer compacted using a tamping rod to minimise air voids. The bottom of each PVC tube was sealed with plastic wrap and cellophane tape to prevent leakage.

After casting, the specimens were left to set for 24 hours. For specimens C and FC, the PVC tubes were removed to produce unconfined specimens. In contrast, specimens TC and FTC retained the PVC tubes as part of the CFPT. To facilitate easy removal, the PVC moulds for C and FC were cut longitudinally and sealed externally with tape prior to casting. This allowed the moulds to maintain their shape during casting and be removed without damaging the specimens. All specimens were cured in a water tank at room temperature for 28 days before mechanical testing.

## Experimental program

The experimental program assessed both material properties and structural performance, as shown in Table 4. Material tests included the slump test (workability), cube compression test (concrete strength), and tensile test (PVC tube strength). These tests confirmed material consistency and provided reference values for all specimen types (C, FC, TC, and FTC).

**Table 4.** Summary of mechanical tests conducted on the specimens.

| Sample | Test Conducted | Purpose | Standard Referred | Testing Equipment |
|---|---|---|---|---|
| Concrete | Slump test | To assess the workability of fresh concrete in each batch | ASTM C143 | Standard slump test set |
| | Cube compression test (150 mm) | To determine the compressive strength of each concrete batch | BS EN 12390-3 | ELE International Compression Machine, ADR Auto V2.0, 2000 kN capacity |
| PVC tube | Tensile test | To measure the tensile strength of the PVC tube | ASTM D638 | Universal Testing Machine, Inspekt 300-1, 300 kN capacity |
| Test specimens | Axial compression test | To determine the compressive strength of specimens C, FC, TC, and FTC | - | Universal Testing Machine, MTS 64.206, 2000 kN capacity |

Axial compression tests, on the other hand, were conducted on all 54 specimens to evaluate the effects of (a) fibre inclusion, (b) fibre content, and (c) PVC confinement on compressive strength. Before testing, each specimen's weight, diameter, and height were measured to ensure dimensional consistency and to calculate axial stress. Testing was performed using a Universal Testing Machine under displacement control at a constant loading rate of 0.10 mm/s until failure. Load and displacement were recorded continuously, and the failure mode was observed.

## RESULTS AND DISCUSSION

### Slump test results

Figures 3 and 4 show that the concrete had low workability, with slump values ranging from 5 mm to 44 mm. This occurred despite a relatively high w/c ratio of 0.58 and the use of a superplasticizer. While such low workability may be acceptable for lightly reinforced foundations [27], it is unsuitable for vertical column casting, where inadequate compaction can lead to honeycombing and compromise structural performance.
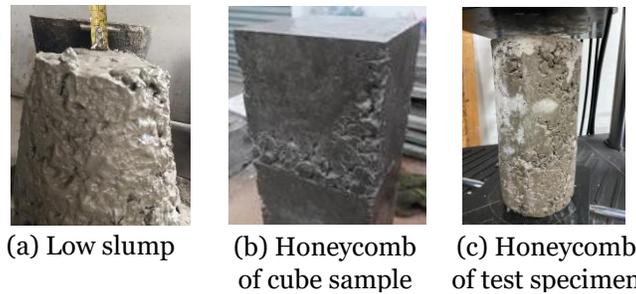
(a) Low slump

(b) Honeycomb of cube sample

(c) Honeycomb of test specimen

**Figure 3.** Concrete exhibiting poor workability due to oven-dried aggregates.



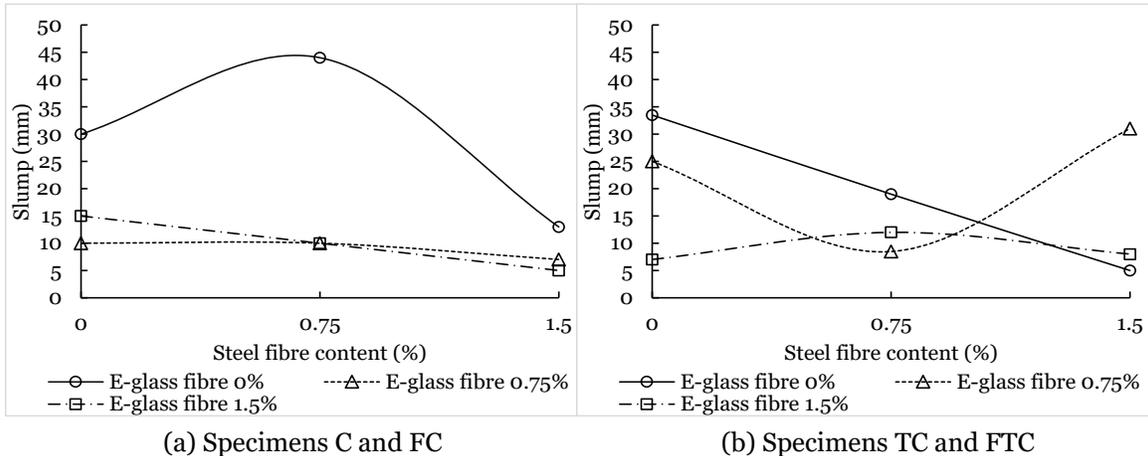(a) Specimens C and FC

(b) Specimens TC and FTC

**Figure 4.** Slump test results indicating fresh concrete workability.

Low workability was likely due to oven-dried aggregates absorbing water and the superplasticizer during mixing. Although oven-dried aggregates helped keep the w/c ratio consistent across batches, they reduced the free water needed for hydration and limited the effectiveness of admixtures. According to [28], aggregates with high water absorption can lower the effective w/c ratio, resulting in poor consistency.

To address this issue, a water absorption test should be done before batching. Knowing the absorption capacity allows for proper water adjustments to ensure enough free water for hydration and admixture effectiveness, improving the workability and consistency of FRC mixes. However, aggregates may not reach full absorption during the short mixing time [28], so it is important to determine the optimal water needed for saturation during concrete mixing and casting.

Workability was reduced by the inclusion of steel and E-glass fibres. Plain concrete mixes (C-1 and TC-1) had higher slump values than those with fibres (Figure 4). Fibre addition increases the surface area needing wetting, reducing the free water available to lubricate cement particles [29]. Fibres also raise internal friction and hinder the flow of fresh concrete [30]. This reduction in workability was more pronounced with higher fibre content or the use of mixed fibre types. Similar observations were reported by [31] and [32], who found that workability decreased with fibre inclusion, particularly at higher fibre contents.

Low workability affects fibre dispersion, increasing the risk of segregation and entanglement [29]. This makes concrete harder to place and compact, leading to honeycombing and air voids, as seen in Figure 3(b) and Figure 3(c). These defects reduce the load-bearing area and cause stress concentrations.

## Cube compressive test results

Table 5 shows that cube compressive strength was consistent across all batches. The COV values for most specimens were below 10%, indicating good repeatability, although FTC-2 exhibited a higher COV of 20.8%, likely due to uneven fibre distribution. All specimens met the target strength of 25 N/mm². Specimen FTC-

8 recorded a 24.6 N/mm², slightly below but still close to the targeted strength. Overall, strength values were higher than the design strength because the mix design was based on a higher target mean strength (38.12 N/mm²), following standard procedures. This ensures a 95% confidence level that the specified strength will be achieved under field conditions.

**Table 5.** Compressive strength results of concrete cubes at 28 days.

| Specimen | Cube 1 (N/mm²) | Cube 2 (N/mm²) | Cube 3 (N/mm²) | Average strength (N/mm²) | Standard Deviation (N/mm²) | Coefficient of Variation (%) |
|---|---|---|---|---|---|---|
| C-1 | 39 | 37 | 35.3 | 37.1 | 1.85 | 5.0 |
| FC-1 | 27.9 | 33 | 31.2 | 30.7 | 2.59 | 8.4 |
| FC-2 | 33.6 | 34.5 | 35 | 34.4 | 0.71 | 2.1 |
| FC-3 | 30.4 | 34.4 | 30.5 | 31.8 | 2.28 | 7.2 |
| FC-4 | 35.4 | 33.1 | 34.3 | 34.3 | 1.15 | 3.4 |
| FC-5 | 31 | 32.6 | 31.1 | 31.6 | 0.9 | 2.8 |
| FC-6 | 33 | 33.8 | 33.9 | 33.6 | 0.49 | 1.5 |
| FC-7 | 34.5 | 36.4 | 33.8 | 34.9 | 1.35 | 3.9 |
| FC-8 | 27.2 | 29.8 | 36.3 | 31.1 | 4.69 | 15.1 |
| TC-1 | 36.3 | 34.3 | 30.5 | 33.7 | 2.95 | 8.8 |
| FTC-1 | 30.7 | 36.5 | 29 | 32.1 | 3.93 | 12.2 |
| FTC-2 | 26.8 | 28.8 | 39 | 31.5 | 6.54 | 20.8 |
| FTC-3 | 31.4 | 29.1 | 29 | 29.8 | 1.36 | 4.6 |
| FTC-4 | 28.9 | 30.7 | 27.5 | 29.0 | 1.6 | 5.5 |
| FTC-5 | 35.1 | 34.6 | 34.2 | 34.6 | 0.45 | 1.3 |
| FTC-6 | 27.5 | 30.2 | 28.9 | 28.9 | 1.35 | 4.7 |
| FTC-7 | 35.1 | 28.5 | 29.8 | 31.1 | 3.5 | 11.3 |
| FTC-8 | 24.1 | 24.7 | 25 | 24.6 | 0.46 | 1.9 |

The improved strength may also be due to a lower effective w/c ratio, caused by partial absorption of mixing water by oven-dried aggregates. The reduction in free water limits capillary pore formation, which results in a denser microstructure and higher compressive strength, provided that workability is adequate. [33] reported that a w/c ratio of 0.3 produced the best mortar performance, with lower ratios reducing porosity.

## Tensile strength of PVC tube

Table 6 presents the tensile strength of the PVC tubes, with an average ultimate strength of 28.8 N/mm². The results from the three samples were consistent, indicating uniform material quality.

**Table 6.** Mechanical properties of polyvinyl chloride (PVC) tubes.

| Specimen | Area (mm²) | Yield load (N) | Yield strength (N/mm²) | Ultimate load (N) | Ultimate strength (N/mm²) |
|---|---|---|---|---|---|
| S1 | 27.02 | 689.7 | 25.5 | 755.7 | 28.0 |
| S2 | 26.11 | 697.9 | 26.7 | 762.3 | 29.2 |
| S3 | 29.11 | 774.3 | 26.6 | 848.4 | 29.1 |
| Average | - | - | 26.3 | - | 28.8 |

Compared to steel, which typically has a tensile strength of 250–300 N/mm², PVC has much lower tensile strength. Consequently, the confinement provided by PVC tubes is weaker than that of steel tubes. [34] noted that the confining effect of UPVC is similar to PVC but significantly lower than that of steel.

This limitation can be reduced by increasing the tube thickness. [9] reported that thicker PVC tubes improve the axial strength and ductility of concrete-filled tubes. Similarly, [35] found that increasing UPVC tube thickness enhances the load-carrying capacity of both plain and fibre-reinforced concrete, although the improvement was marginal due to the material's low stiffness.

## Axial compression test

Axial compression tests were carried out on specimens C, FC, TC, and FTC to measure compressive strengths. Each group included three specimens with consistent dimensions (Table 7). Specimens without PVC tubes (C and FC) weighed 12.82–13.6 kg, while those with PVC tubes (TC and FTC) weighed 13.32–14.36 kg. All specimens were approximately 305 mm in height. C and FC had a diameter of 155 mm, and TC and FTC had a diameter of 159 mm due to the 2 mm thick PVC tubes. Dimensional consistency was high, with weight COV of 0.3–3.0%, diameter COV of 0%, and height COV of 0.2–1.8%, ensuring that variations in compressive strength reflected material and confinement effects rather than specimen irregularities.

**Table 7.** Final dimensions of specimens after casting and curing.

| Specimen | Average weight (kg) | SD (kg) | COV (%) | Average diameter, $d$ (mm)* | Average height, $h$ (mm) | SD (mm) | COV (%) |
|---|---|---|---|---|---|---|---|
| C-1 | 13.5 | 0.12 | 0.9 | 155 | 304.7 | 0.6 | 0.2 |
| FC-1 | 13.51 | 0.09 | 0.7 | 155 | 302.0 | 1.0 | 0.3 |
| FC-2 | 13.41 | 0.15 | 1.1 | 155 | 302.7 | 1.5 | 0.5 |
| FC-3 | 13.6 | 0.18 | 1.3 | 155 | 306.3 | 3.5 | 1.1 |
| FC-4 | 13.01 | 0.09 | 0.7 | 155 | 302.7 | 2.9 | 1.0 |
| FC-5 | 13.36 | 0.12 | 0.9 | 155 | 304.3 | 4.9 | 1.6 |
| FC-6 | 12.82 | 0.12 | 0.9 | 155 | 303.7 | 1.2 | 0.4 |
| FC-7 | 13.28 | 0.14 | 1.1 | 155 | 303.7 | 5.5 | 1.8 |
| FC-8 | 13.02 | 0.09 | 0.7 | 155 | 301.7 | 2.9 | 1.0 |
| TC-1 | 14.15 | 0.04 | 0.3 | 159 | 303.0 | 1.7 | 0.6 |
| FTC-1 | 14.36 | 0.31 | 2.2 | 159 | 304.0 | 5.3 | 1.7 |
| FTC-2 | 14.06 | 0.10 | 0.7 | 159 | 303.3 | 1.2 | 0.4 |
| FTC-3 | 14.31 | 0.32 | 2.2 | 159 | 307.7 | 3.2 | 1.0 |
| FTC-4 | 13.5 | 0.41 | 3.0 | 159 | 304.0 | 3.5 | 1.2 |
| FTC-5 | 13.53 | 0.25 | 1.8 | 159 | 305.7 | 3.5 | 1.1 |
| FTC-6 | 13.32 | 0.40 | 3.0 | 159 | 304.3 | 4.0 | 1.3 |
| FTC-7 | 13.76 | 0.15 | 1.1 | 159 | 301.7 | 1.5 | 0.5 |
| FTC-8 | 13.73 | 0.05 | 0.4 | 159 | 302.7 | 2.1 | 0.7 |

*Note: Standard deviation (SD) and coefficient of variation (COV) for specimen diameter are zero because the measured diameters were constant across all specimens.

Figure 5 demonstrates the load-displacement curves of representative specimens for C, FC, TC, and FTC. The ultimate load was obtained as the peak of each curve, representing the maximum load recorded by the Universal Testing Machine. The average ultimate load, $P_u$, was calculated from three specimens per group and is summarized in Table 8. Variability was observed in the results, with COV ranging from 2.4% to 35.4%. Twelve of the eighteen specimens exhibited COV exceeding 10%, likely due to low workability and variations in compaction quality.
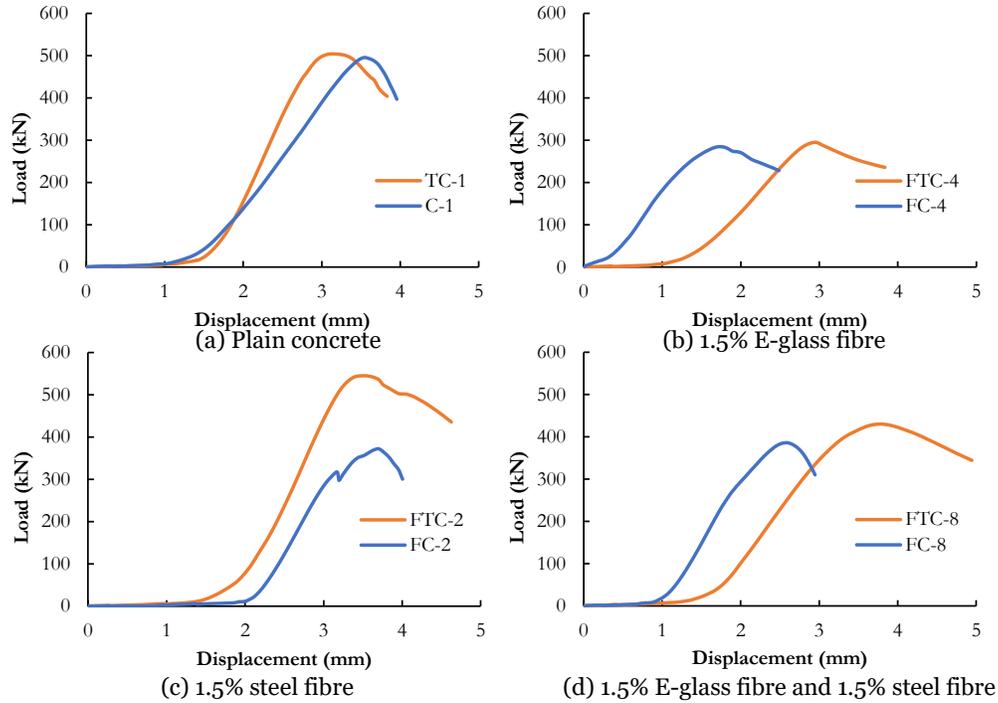
**Figure 5.** Load-displacement response of specimens.

**Table 8.** Axial compression test results for specimens C, FC, TC, and FTC.

| Specimen | Concrete Grade, $f_c$ (N/mm²) | Ultimate load | | | | | | Average Compressive Stress, $f_u$ (N/mm²) |
| --- | --- | --- | --- | --- | --- | --- | --- | --- |
| | | Sample 1 (kN) | Sample 2 (kN) | Sample 3 (kN) | Average, $P_u$ (kN) | SD (kN) | COV (%) | |
| C-1 | 37.1 | 475.2 | 514.6 | 495.8 | 495.2 | 19.7 | 4 | 26.2 |
| FC-1 | 30.7 | 508.3 | 440.5 | 418.7 | 455.8 | 46.7 | 10.2 | 24.2 |
| FC-2 | 34.37 | 371.9 | 256.8 | 450 | 359.6 | 97.2 | 27 | 19.1 |
| FC-3 | 31.77 | 253.2 | 177.6 | 292 | 240.9 | 58.2 | 24.2 | 12.8 |
| FC-4 | 34.27 | 188.3 | 273.5 | 285.1 | 249 | 52.9 | 21.2 | 13.2 |
| FC-5 | 31.57 | 474.2 | 369 | 308.2 | 383.8 | 84 | 21.9 | 20.3 |
| FC-6 | 33.57 | 188.3 | 351.6 | 276.8 | 272.2 | 81.7 | 30 | 14.4 |
| FC-7 | 34.9 | 241 | 343.1 | 307.5 | 297.2 | 51.8 | 17.4 | 15.8 |
| FC-8 | 31.1 | 288 | -* | 386.2 | 337.1 | 69.4 | 20.6 | 17.9 |
| TC-1 | 33.7 | 518.6 | 503.9 | 495 | 505.8 | 11.9 | 2.4 | 25.5 |
| FTC-1 | 32.07 | 501.9 | 301.1 | -* | 401.5 | 142 | 35.4 | 20.2 |
| FTC-2 | 31.53 | 497.4 | -* | 544.9 | 521.2 | 33.6 | 6.4 | 26.2 |
| FTC-3 | 29.83 | 305.2 | 399 | 534.6 | 412.9 | 115.3 | 27.9 | 20.8 |
| FTC-4 | 29.03 | 295.3 | 331.2 | 341.1 | 322.5 | 24.1 | 7.5 | 16.2 |
| FTC-5 | 34.63 | 305.4 | 246.1 | 249 | 266.8 | 33.4 | 12.5 | 13.4 |
| FTC-6 | 28.87 | 221.2 | 201.9 | 363.8 | 262.3 | 88.4 | 33.7 | 13.2 |
| FTC-7 | 31.13 | 418.9 | 506.5 | 455.6 | 460.3 | 44 | 9.6 | 23.2 |
| FTC-8 | 24.6 | 454.2 | 393 | 430.1 | 425.8 | 30.8 | 7.2 | 21.4 |

*Note: Results for these specimens were unavailable due to an unexpected failure detected by the testing machine, which prevented valid data acquisition.

A higher variability was observed in the compressive strength of the cylinder and CFPT specimens (COV 2.4%–35.4%, Table 8) compared to the cube specimens (COV 1.3%–20.8%, Table 5), despite using the same mix. This difference likely arose because the cylinders and CFPTs, having higher aspect ratios, were more sensitive to compaction quality, fibre dispersion, end friction, and loading alignment. Small inconsistencies in these factors could have caused larger scatter in the results, reflected by higher COV values. In contrast, the cubes were less affected by such factors due to their lower aspect ratio and simpler geometry. Additionally, the cubes were cast immediately after mixing, while the cylinders and CFPTs were prepared later. As a result, a portion of the mix might have lost workability over time, especially in fibre-reinforced batches, leading to reduced compaction efficiency and greater variability in the latter specimens.

The average compressive stress ($f_u$) was calculated by dividing $P_u$ by the total cross-sectional area, assuming that both the concrete and PVC tubes shared the axial load equally. Since specimen diameters differed (155 mm for C and FC, 159 mm for TC and FTC), $f_u$ provides a consistent basis for comparison. The $f_u$ was then organized according to the percentage of steel and E-glass fibre inclusion to illustrate the parametric response, as presented in Table 9.

**Table 9.** Average ultimate stress, $f_u$, for each specimen (N/mm$^2$).

| E-glass Fibre Content | Without PVC tube (unconfined state) | | | With PVC tube (confined state) | | |
|---|---|---|---|---|---|---|
| | Steel fibre content | | | Steel fibre content | | |
| | 0 | 0.75% | 1.50% | 0 | 0.75% | 1.50% |
| 0 | 26.2 | 24.2 | 19.1 | 25.5 | 20.2 | 26.2 |
| 0.75% | 12.8 | 20.3 | 15.8 | 20.8 | 13.4 | 23.2 |
| 1.50% | 13.2 | 14.4 | 17.9 | 16.2 | 13.2 | 21.4 |

The comparison between C-1 and TC-1 highlights the limited effect of PVC tube confinement on plain concrete. TC-1 reached a slightly higher ultimate load ($P_u$ = 505.8 kN) than C-1 (495.2 kN), but the improvement in compressive stress was minimal. Removing the tube after casting left C-1 carrying the entire load on concrete alone, with a smaller effective cross-sectional area, resulting in a higher ultimate stress ($f_u$). In TC-1, load sharing with the low-stiffness, thin-walled PVC tube, combined with its limited hoop tensile strength, produced only a marginal increase in compressive stress. The limited effect is further evident in fibre-reinforced specimens: FTC-1, FTC-5, and FTC-6 exhibited lower $f_u$ than their unconfined counterparts, while FTC-2, FTC-3, FTC-4, FTC-7, and FTC-8 showed higher $f_u$.

Fibre addition did not improve compressive strength, whether or not with tube confinement. Among the unconfined specimens, plain concrete (C-1) showed the highest compressive stress at 26.2 N/mm$^2$, while fibre-reinforced specimens (FC-1 to FC-8) ranged from 12.8 to 24.2 N/mm$^2$. This suggests that adding E-glass fibres, steel fibres, or both generally reduced compressive strength. Under confinement, only specimen FTC-2 (with 1.5% steel fibres and 0% E-glass fibres) outperformed TC-1 (plain concrete with tube), indicating minimal benefit from fibre inclusion.

However, these findings differ from previous studies. [35] reported that FRC confined in UPVC pipes had higher load capacity than plain concrete, with improved ductility and gradual post-peak strength loss. Similarly, [32] found that adding 1.25% glass fibre increased the compressive strength of self-compacting concrete by up to 47.92%, but no further gain was observed when the fibre content was raised from 1.5% to 2.5%. [36] reported that adding steel fibres had a moderate effect on the ultimate strength of CFST columns but significantly improved ductility, due to increased compressive ductility and post-cracking tensile strength. These studies suggest that fibres consistently enhance ductility more than compressive strength.

The reduction in compressive strength due to fibre inclusion may be attributed to several factors. Poor fibre dispersion or clumping could have disrupted the concrete matrix, creating weak zones and stress concentrations that reduced its load-bearing capacity. Additionally, the lower workability resulting from fibre addition may have hindered proper compaction, leading to internal voids and honeycombing that further weakened the concrete. Moreover, using fibre content beyond the optimal level likely caused severe workability loss and increased clumping, ultimately outweighing any potential reinforcing benefits.

These observations are consistent with the findings of [37], who reported that decreased compressive strength may result from fibre aggregation (clumping) and reduced workability, which can lead to entrapped air. Similarly, [32] found that higher doses of glass fibres slightly reduce the mechanical performance of concrete due to poor workability.

Compared to steel fibres, E-glass fibres caused a greater reduction in compressive strength. When E-glass fibre content increased from 0% to 1.5%, compressive strength dropped by 49.6% in unconfined specimens and 36.5% in confined specimens (as seen in specimens C-1, FC-4, TC-1, and FTC-4). In contrast, increasing steel fibre content from 0% to 1.5% led to a 27.1% strength reduction in unconfined specimens, but a slight 2.7% increase in confined specimens (specimens C-1, FC-2, TC-1, and FTC-2).

The stronger negative impact of E-glass fibres compared to steel fibres may be explained by several factors. The lower stiffness and tensile strength of E-glass fibres make them less effective at bridging microcracks and resisting compressive forces. Their smooth surface also results in weaker bonding with the cement matrix, offering less mechanical interlock than steel fibres. Additionally, the higher fineness and electrostatic properties of E-glass fibres increase their tendency to clump during mixing, leading to poor dispersion, internal voids, and the formation of local weak zones.

Combining steel and E-glass fibres reduced compressive strength in both confined and unconfined concrete. For instance, FC-8 and FTC-8 showed 31.7% and 16.1% lower strength than plain concrete (C-1 and TC-1). As E-glass fibre content increased from 0% to 1.5%, strength consistently declined, even with steel fibres. Specimens FTC-4, FTC-6, and FTC-8 (each with 1.5% E-glass fibres) showed strength reductions of 36.5%, 34.7%, and 18.3% compared to specimens without E-glass fibres. In contrast, increasing steel fibre content slightly improved strength when E-glass fibres were present. FTC-2, FTC-7, and FTC-8 recorded strength increases of 2.7%, 11.5%, and 32.1% compared to specimens with 0% steel fibres.

Steel and E-glass fibres did not work well together. While steel fibres enhanced the strength of concrete with E-glass fibres, E-glass fibres reduced the strength of concrete with steel fibres. This may be due to the poor distribution of E-glass fibres, which disrupts the bond between steel fibres and the cement matrix, thereby weakening crack control. The lower stiffness and poor bonding characteristics of E-glass fibres may also dominate the overall mix behaviour, offsetting the benefits provided by steel fibres. Furthermore, the combined fibre content of up to 3% likely exceeded the optimal limit, reducing workability, causing poor dispersion, and ultimately weakening the concrete matrix.

According to [34], using excessive amounts of polypropylene (PP) fibres (>1 kg/m³) can reduce the axial load capacity of CFPTs made of UPVC. [38] also reported that higher fibre content increases fibre concentration and the likelihood of fibre clustering, which can further weaken the concrete.

Some specimens with PVC tubes, such as FTC-2, FTC-3, FTC-4, FTC-7, and FTC-8, showed higher compressive strength than their unconfined counterparts (Table 9). However, others like TC-1, FTC-1, FTC-5, and FTC-6 recorded lower strength. This shows that PVC tube confinement did not consistently enhance performance.

Several factors may explain this outcome. The PVC tubes had low tensile strength (28.8 N/mm²) and thin walls (2 mm); compared to steel, PVC provides much lower stiffness and hoop strength, which limits its ability to resist lateral dilation and deliver effective confinement. Poor workability and compaction, particularly inside the tube, may also have resulted in internal voids or honeycombing, defects that not only reduce compressive strength but also weaken the interaction between the concrete core and the confining tube. Additionally, confinement depends on the concrete's lateral expansion to activate hoop stress, but in stiff or low-workability mixes, this expansion may be too limited or occur too late to fully engage the tube before the peak load is reached.

[39] noted that when the steel tube expands more than the concrete, the confinement effect is delayed. This causes delamination at the interface between the steel tube and the core concrete, leaving the concrete core unconfined until cracks form and its lateral expansion exceeds that of the steel tube.

## Failure mode

Unconfined specimens (C and FC) experienced elastic shortening and lateral expansion under compression. Once the concrete's deformability was exceeded, micro-cracks formed at the interface between the cement

matrix and aggregates. These micro-cracks gradually extended and merged into larger localized cracks. With continued loading, localized crushing, spalling, and vertical splitting cracks developed, eventually leading to failure (Figure 6).
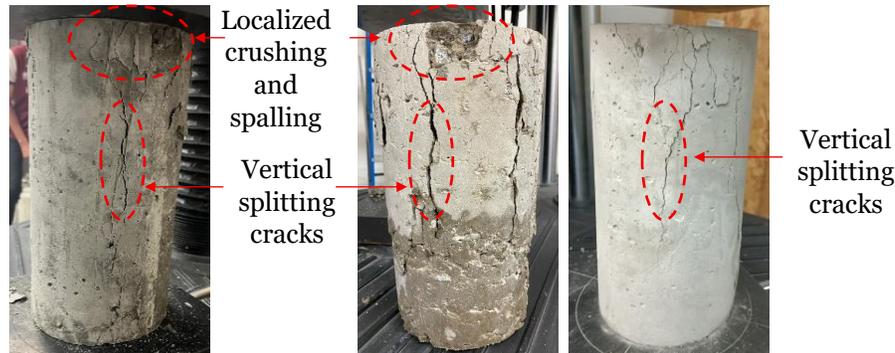


**Figure 6.** Typical failure patterns observed in unconfined specimens C and FC.

These failure modes highlight the importance of resisting lateral expansion to delay or prevent compressive failure. This resistance can theoretically be achieved by (a) reinforcing concrete with fibres, and/or (b) providing confinement using tubes.

Fibres can resist lateral expansion by bridging micro-cracks and controlling their growth. As cracks form under load, fibres transfer tensile stress across the crack faces, delaying their widening and limiting deformation. This bridging action enhances post-cracking behaviour and ductility. However, the effectiveness depends on the fibre type, volume, orientation, and bond with the cement matrix. In this study, both steel and E-glass fibres did not consistently improve compressive strength. Most of the fibre-reinforced concrete specimens (FC-1 to FC-8 and FTC-1 to FTC-8) recorded lower strength than plain concrete (C-1 and TC-1) (Table 9). This may be due to incompatible fibre combinations or excessive total fibre content, which can reduce workability and compromise strength.

Tube confinement works by restraining the lateral expansion of concrete under compression. As the concrete expands, it activates hoop stress in the surrounding tube, which resists further dilation. However, because this mechanism is passive, it does not prevent the initiation of micro-cracks but may limit their excessive growth. Confinement only becomes effective once the lateral expansion of the concrete exceeds that of the tube.

The effectiveness of tube confinement depends on material properties, wall thickness, and the presence of any gap between the concrete and the tube. In this study, the PVC tube had a low tensile strength (28.8 N/mm²), thin walls (2 mm), and low stiffness, offering limited confinement before peak strength. This resulted in inconsistent strength improvement, as seen in the comparison of specimens C and FC (unconfined) with TC and FTC (confined): 5 showed strength gains, while 4 showed reductions (Table 9).

The failure modes of the confined specimens (TC and FTC), such as significant deformation of the PVC tubes resulting from excessive concrete dilation or shear failure, support this observation (Figure 7).



**Figure 7.** Typical failure patterns observed in confined specimens TC and FTC.

Due to the stiff, low-workability concrete, lateral expansion was often insufficient to activate confinement before failure, highlighting the delayed response and limited effectiveness of PVC tubes in this setup.

## Limitations and Recommendations

This study has several limitations, and the conclusions should be validated through future research. The observed reduction in compressive strength suggests that steel fibres, E-glass fibres, or their combination may not be suitable for reinforcing concrete infill in CFPTs with PVC tubes. However, this strength loss could also be attributed to poor workability or uneven fibre distribution. The experimental setup did not include methods to distinguish between these effects, so it remains unclear whether the reduction was caused by the fibres or the quality of the concrete mix.

No tests were conducted to confirm fibre clumping or to assess the bond between the fibres and the cement matrix. The explanation for poor performance was either speculation or inferred from previous studies rather than supported by direct evidence. Therefore, the possible causes remain uncertain.

The study also did not determine the optimum fibre dosage. All mixes used 0%, 0.75%, and 1.5% by cement weight for each fibre type. In hybrid mixes, the total dosage reached 3%, which may have exceeded the optimal level. Due to the significantly lower density of E-glass fibres compared to steel fibres, equal weight percentages resulted in a much higher volume of E-glass, increasing the risk of overdosage. This likely reduced workability and strength, especially in mixes containing E-glass fibres. Future studies should consider lower dosages for E-glass fibres and ensure that the total fibre content in hybrid mixes does not exceed the maximum for a single fibre type.

To improve future outcomes, studies should include better control of workability, direct assessment of fibre distribution and bonding (e.g. through microstructural analysis), and more appropriate dosage ranges. These improvements would help clarify the individual and combined effects of fibres on CFPT performance.

Fibres in concrete primarily enhance crack resistance and post-cracking ductility, with more significant effects under tension than compression. Their contribution to compressive strength is typically marginal. The strength reduction observed in this study likely resulted from a combination of factors: oven-dried aggregates that reduced workability and compaction, high or uneven fibre dosage that caused fibre clumping and voids, and weak PVC confinement that provided limited lateral restraint. These factors may have overshadowed the potential benefits of fibre reinforcement and confinement. Consequently, the findings do not conclusively represent the true compressive behaviour of FRC in CFPTs but rather the influence of these methodological constraints. Future work should better control these parameters to isolate and quantify the actual contribution of FRC to confined compressive performance.

Lateral strain data was not recorded in this study, preventing direct evaluation of the confinement mechanism provided by the PVC tube. Future work should include both axial and lateral strain measurements to quantify confinement efficiency and validate stress-strain behaviour.

This study also did not assess ductility or toughness, which require post-peak stress-strain data. These parameters were excluded to maintain focus on compressive strength and failure modes. Future studies should include post-peak analysis to evaluate the deformation capacity and energy absorption characteristics of CFPTs.

## CONCLUSION

This study examined the effects of steel and E-glass fibres on the compressive strength of concrete-filled PVC tubes. A total of 54 specimens were tested across four groups: plain concrete (C), fibre-reinforced concrete (FC), concrete-filled PVC tubes (TC), and fibre-reinforced concrete-filled PVC tubes (FTC). All specimens used consistent material properties and dimensions, but the concrete had low workability, which may have affected casting quality and strength.

Fibre addition generally did not improve compressive strength. Only one specimen (FTC-2) with 1.5% steel fibres showed a marginal increase of 2.7. E-glass fibres caused greater strength reductions than steel fibres, especially in unconfined specimens. Increasing E-glass content from 0% to 1.5% reduced

compressive strength by 49.6% in unconfined specimens and 36.5% in confined ones. Increasing steel fibres led to a 27.1% reduction in unconfined specimens but a 2.7% gain in confined ones. The combination of both fibres did not improve compressive strength under the mix conditions used, likely due to poor fibre distribution, the low stiffness of E-glass fibres, and excessive fibre content, which reduced workability.

PVC tube confinement produced inconsistent results. Five specimens gained strength, while four showed reductions. This was likely due to the tube's low tensile strength and thin walls, which offered limited confinement before failure. These findings suggest that hybrid fibre reinforcement in low-workability concrete, especially when combined with weak confinement, may not provide strength benefits.

Low concrete workability remains a key limitation of this study. Fibre dispersion and bonding were not directly assessed, making it unclear whether the strength reductions were caused by the fibres or poor mix quality. Future research should include better control of workability, direct evaluation of fibre distribution and bonding through techniques such as microstructural analysis, and more suitable fibre dosage levels, particularly in hybrid mixes.

## ACKNOWLEDGEMENT

## CONFLICT OF INTEREST

The authors declare no conflict of interest.

## REFERENCES

[1] Azeez, A. A., Jamaluddin, N., Rahman, N. A., Hassen, D. R., and Attiyah, A. N. (2018). Experimental and analytical study of PVC confined concrete cylinders. *J. Eng. Appl. Sci.*, 13(8): 2145–2151. doi: 10.36478/jeasci.2018.2145.2151.

[2] Wang, X., Fan, F., and Lai, J. (2022). Strength behavior of circular concrete-filled steel tube stub columns under axial compression: A review. *Constr. Build. Mater.*, 322: 126144. doi: 10.1016/j.conbuildmat.2021.126144.

[3] He, L., Zhao, Y., and Lin, S. (2018). Experimental study on axially compressed circular CFST columns with improved confinement effect. *J. Constr. Steel Res.*, 140: 74–81. doi: 10.1016/j.jcsr.2017.10.025.

[4] Zhao, X.-L., and Han, L.-H. (2006). Double skin composite construction. *Prog. Struct. Eng. Mater.*, 8(3): 93–102. doi: 10.1002/pse.216.

[5] Han, L.-H., Li, W., and Bjorhovde, R. (2014). Developments and advanced applications of concrete-filled steel tubular (CFST) structures: Members. *J. Constr. Steel Res.*, 100: 211–228. doi: 10.1016/j.jcsr.2014.04.016.

[6] Fakharifar, M., and Chen, G. (2017). FRP-confined concrete filled PVC tubes: A new design concept for ductile column construction in seismic regions. *Constr. Build. Mater.*, 130: 1–10. doi: 10.1016/j.conbuildmat.2016.11.056.

[7] Cao, V. V., Le, Q. D., and Nguyen, P. T. (2020). Experimental behaviour of concrete-filled steel tubes under cyclic axial compression. *Adv. Struct. Eng.*, 23(1): 74–88. doi: 10.1177/1369433219866107.

[8] Katsimpini, P., Papagiannopoulos, G., and Hatzigeorgiou, G. (2024). A simple method to evaluate the bearing capacity of concrete-filled steel tubes with rectangular and circular sections: Beams, columns, and beam–columns. *Appl. Sci.*, 14(19): 8995.

[9] Wang, J.-Y., and Yang, Q.-B. (2012). Investigation on compressive behaviors of thermoplastic pipe confined concrete. *Constr. Build. Mater.*, 35: 578–585. doi: 10.1016/j.conbuildmat.2012.04.017.

[10] Li, G., Hou, C., Shen, L., and Yao, G.-H. (2022). Performance and strength calculation of CFST columns with localized pitting corrosion damage. *J. Constr. Steel Res.*, 188: 107011. doi: 10.1016/j.jcsr.2021.107011.

[11] Melchers, R. E. (2006). Recent progress in the modeling of corrosion of structural steel immersed in seawaters. *J. Infrastruct. Syst.*, 12(3): 154–162. doi: 10.1061/(ASCE)1076-0342(2006)12:3(154).

[12] Mohamed, H. M., and Masmoudi, R. (2010). Axial load capacity of concrete-filled FRP tube columns: Experimental versus theoretical predictions. *J. Compos. Constr.*, 14(2): 231–243. doi: 10.1061/(ASCE)CC.1943-5614.0000066.

[13] Ozbakkaloglu, T. (2013). Axial compressive behavior of square and rectangular high-strength concrete-filled FRP tubes. *J. Compos. Constr.*, 17(1): 151–161. doi: 10.1061/(ASCE)CC.1943-5614.0000321.

[14] Ozbakkaloglu, T. (2013). Concrete-filled FRP tubes: Manufacture and testing of new forms designed for improved performance. *J. Compos. Constr.*, 17(2): 280–291. doi: 10.1061/(ASCE)CC.1943-5614.0000334.

[15] Deng, J., Zheng, Y., Wang, Y., Liu, T., and Li, H. (2017). Study on axial compressive capacity of FRP-confined concrete-filled steel tubes and its comparisons with other composite structural systems. *Int. J. Polym. Sci.*, 2017: 6272754. doi: 10.1155/2017/6272754.

[16] Chen, G. M., Lan, Z. H., Xiong, M. X., and Xu, Z. (2020). Compressive behavior of FRP-confined steel-reinforced high strength concrete columns. *Eng. Struct.*, 220: 110990. doi: 10.1016/j.engstruct.2020.110990.

[17] Lu, Y., Li, N., and Li, S. (2014). Behavior of FRP-confined concrete-filled steel tube columns. *Polymers*, 6(5): 1333–1349. doi: 10.3390/polym6051333.

[18] Abbood, I. S., Odaa, S. A., Hasan, K. F., and Jasim, M. A. (2021). Properties evaluation of fiber reinforced polymers and their constituent materials used in structures – A review. *Mater. Today Proc.*, 43: 1003–1008. doi: 10.1016/j.matpr.2020.07.636.

[19] Abdulla, N. A. (2017). Concrete filled PVC tube: A review. *Constr. Build. Mater.*, 156: 321–329. doi: 10.1016/j.conbuildmat.2017.08.156.

[20] Nunna, S., Ravindran, A. R., Mroszczok, J., Creighton, C., and Varley, R. J. (2023). A review of the structural factors which control compression in carbon fibres and their composites. *Compos. Struct.*, 303: 116293. doi: 10.1016/j.compstruct.2022.116293.

[21] Ling, J. H., Lim, Y. T., Leong, W. K., and Sia, H. T. (2023). Concrete-filled tubular column made of various types of material. *J. Civil Eng.*, 38(1): 3–15. doi: 10.12962/j20861206.v38i1.15455.

[22] Fakharifar, M., and Chen, G. (2016). Compressive behavior of FRP-confined concrete-filled PVC tubular columns. *Compos. Struct.*, 141: 91–109. doi: 10.1016/j.compstruct.2016.01.004.

[23] Vairagade, V. S., and Dhale, S. A. (2023). Hybrid fibre reinforced concrete – A state of the art review. *Hybrid Adv.*, 3: 100035. doi: 10.1016/j.hybadv.2023.100035.

[24] Lu, Y., Li, N., Li, S., and Liang, H. (2015). Behavior of steel fiber reinforced concrete-filled steel tube columns under axial compression. *Constr. Build. Mater.*, 95: 74–85. doi: 10.1016/j.conbuildmat.2015.07.114.

[25] Labib, W. (2015). An overview into the use of single and hybrid fibre reinforced concrete. *In 8th Int. Conf. Fibre Concrete 2015*, Prague, Czech Republic.

[26] Abadel, A., Abbas, H., Almusallam, Al-Salloum, T., Y. and Siddiqui, N. (2015). Mechanical properties of hybrid fibre-reinforced concrete – Analytical modelling and experimental behaviour. *Mag. Concr. Res.*, 68(16): 823–843. doi: 10.1680/jmacr.15.00276.

[27] Gilson Company Inc. (n.d.). *Concrete slump testing: Test methods, equipment, and testing techniques*. [Accessed: 24 Jul. 2025]. Available from: https://www.globalgilson.com/blog/concrete-slump-guide?srsltid=AfmBOoqvlGDhasn8JFmif_ntPGgWZLgHepUl91qV2yBP3oiCrcVzVfIx

[28] Nedeljković, M., Visser, J., Šavija, B., Valcke, S., and Schlangen, E. (2021). Use of fine recycled concrete aggregates in concrete: A critical review. *J. Build. Eng.*, 38: 102196. doi: 10.1016/j.jobe.2021.102196.

[29] Wang, W., Shen, A., Lyu, Z., He, Z., and Nguyen, K. T. Q. (2021). Fresh and rheological characteristics of fiber reinforced concrete – A review. *Constr. Build. Mater.*, 296: 123734. doi: 10.1016/j.conbuildmat.2021.123734.

[30] Pham, T. M. (2025). Fibre-reinforced concrete: State-of-the-art review on bridging mechanism, mechanical properties, durability, and eco-economic analysis. *Case Stud. Constr. Mater.*, 22: e04574. doi: 10.1016/j.cscm.2025.e04574.

[31] Khaloo, A., Molaei Raisi, E., Hosseini, P., and Tahsiri, H. (2014). Mechanical performance of self-compacting concrete reinforced with steel fibers. *Constr. Build. Mater.*, 51: 179–186. doi: 10.1016/j.conbuildmat.2013.10.054.

[32] Ahmad, J., González-Lezcano, R. A., Majdi, A., Ben Kahla, N., Deifalla, A. F., and El-Shorbagy, M. A. (2022). Glass fibers reinforced concrete: Overview on mechanical, durability and microstructure analysis. *Materials*, 15(15): 5111. doi: 10.3390/ma15155111.

[33] Yusslee, E., and Beskhyroun, S. (2023). The effect of water-to-binder ratio (W/B) on pore structure of one-part alkali activated mortar. *Heliyon*, 9(1): e12983. doi: 10.1016/j.heliyon.2023.e12983.

[34] Mohammad Askari, S. M., Khaloo, A., Borhani, M. H., and Tale Masoule, M. S. (2020). Performance of polypropylene fiber reinforced concrete-filled UPVC tube columns under axial compression. *Constr. Build. Mater.*, 231: 117049. doi: 10.1016/j.conbuildmat.2019.117049.

[35] Bandyopadhyay, A., Chanu, Y. M., and Samanta, A. K. (2019). Experimental investigation on mechanical properties of PCC and FRC confined with UPVC pipe. *Indian J. Eng. Mater. Sci.*, 26: 342–348.

[36] Tao, Z., Han, L.-H., and Wang, D.-Y. (2007). Experimental behaviour of concrete-filled stiffened thin-walled steel tubular columns. *Thin-Walled Struct.*, 45(5): 517–527. doi: 10.1016/j.tws.2007.04.003.

[37] Akeed, M. H., Qaidi, S., Ahmed, H. U., Emad, W., Faraj, R. H., Mohammed, A. S., et al. (2022). Ultra-high-performance fiber-reinforced concrete. Part III: Fresh and hardened properties. *Case Stud. Constr. Mater.*, 17: e01265. doi: 10.1016/j.cscm.2022.e01265.

[38] Gao, D., Gu, Z., Wei, C., Wu, C., and Pang, Y. (2021). Effects of fiber clustering on fatigue behavior of steel fiber reinforced concrete beams. *Constr. Build. Mater.*, 301: 124070. doi: 10.1016/j.conbuildmat.2021.124070.

[39] Ekmekyapar, T., and Al-Eliwi, B. J. M. (2017). Concrete filled double circular steel tube (CFDCST) stub columns. *Eng. Struct.*, 135: 68–80. doi: 10.1016/j.engstruct.2016.12.061.